Accepted Manuscript
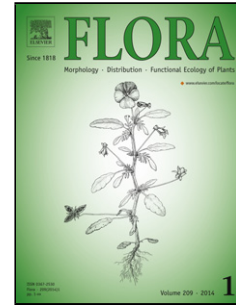
Spatial and temporal variation in volatile composition suggests olfactory division of labor within the trap flowers of *Aristolochia gigantea*

Kyle R. Martin[a], Marcela Moré[b], Juliana Hipólito[c], Shaniece Charlemagne[d,e], Boris O. Schlumpberger[f,g], Robert A. Raguso[f,h]

[a] Department of Plant Biology, Cornell University, Ithaca NY 14853 USA

[b] Laboratorio de Biología Floral, Instituto Multidisciplinario de Biología Vegetal (CONICET-UNCba), CC 10 495, CP 5000, Cordoba, Argentina

[c] Laboratório de Biologia e Ecologia de Abelhas (LABEA), Instituto de Biologia - Departamento de Zoologia, Universidade Federal da Bahia (UFBA), Campus de Ondina CEP 40.170-110 Salvador - BA / Brasil

[d] Department of Chemistry, Benedict College, Columbia SC 29204 USA

[e] Current address: Primary Care Office, US Virgin Islands Department of Health, Charles Harwood Complex, 3500 Est. Richmond, Christiansted, VI 00820 USA

[f] Department of Biological Sciences, University of South Carolina, Columbia SC 29208 USA

[g] Current address: Herrenhäuser Gärten, Herrenhäuser Str. 4, 30419 Hannover, Germany

[h] Current address: Department of Neurobiology and Behavior, Cornell University, Ithaca NY 14853 USA

Highlights

- Floral scent of *Aristolochia gigantea* changes rapidly over its three-day lifespan.
- Distinct spatial units within the flower release markedly different volatile blends.
- A function to choreograph pollinator behavior to mediate pollen transfer is posited.

Abstract

The olfactory components of floral advertisement can be complex, often showing dynamic patterns of emission and chemical composition that may reflect diverse functions related to pollination. In this study we investigated the spatial and temporal variation of volatile production in the distinctive kettle trap flowers of the Neotropical pipevine *Aristolochia gigantea* (Aristolochiaceae). These flowers show unusual complexity in scent chemistry and floral morphology in addition to conspicuous changes in scent at distinct stages during floral ontogeny. In this study, volatiles were collected from separate stages in development (bud, female, male, wilted flower), and from different functional units (limb, black ring, yellow disk, utricle, nectary) within each stage. Our results document a strikingly complex and dynamic floral scent composition for *A. gigantea*. Female stage floral emissions are dominated by sweet lemon-scented citronella-like compounds including (*E*)- and (*Z*)-citral, citronellol and citronellal, and at the same time include smaller amounts of pungent, brood-site associated volatiles such as dimethyl disulfide, 2-heptanone, and 3-methyl-1-butanol. Volatile emissions plummet one day later in male stage flowers, except for increased production of monoterpenoids and sesquiterpenoids, including a burst of linalool within the floral chamber. Volatiles emitted from wilted flowers resemble the vegetative background as soon as 48 hours post

2

anthesis. Multidimensional scaling revealed unexpected differentiation of volatile emissions across spatial units of the complex flower (e.g. within vs. outside of the trap), as well as at different stages of sexual expression as flowers matured. These results suggest that protogynous kettle trap flowers or inflorescences utilize a chemical division of labor, in concert with visual and tactile cues, to choreograph pollinator behavior such that female and male floral functions are optimized.

Key words: brood site deception, floral scent, fly pollination, kettle trap flower, Phoridae, protogyny

1. Introduction

Flowers advertise to their animal visitors through a sophisticated interplay of visual, olfactory and other sensory stimuli whose primary functions are to attract pollinators and manipulate their behavior in ways that mediate pollen transfer (Dobson, 1994; Leonard et al., 2011). The olfactory components of floral advertisement can be highly complex, exhibiting dynamic patterns of emission and chemical composition that may reflect diverse functions regarding pollinator behavior (Raguso, 2008; Wright and Schiestl, 2009). For example, specific components of a floral scent blend can function as long distance attractants, while others may induce feeding or signal the presence of a floral reward, among other functions (Dobson et al., 1996; Dötterl and Jürgens, 2005). Although flower petals often are the primary source of floral scent, volatile emissions are known to vary spatially among different floral organs (Dobson et al., 1990; Effmert et al.,

2006) and can in some cases be localized to glandular regions within such organs, described by Vogel (1963) as "osmophores".

Floral scent also varies temporally, due to a variety of physiological and ecological causes (Proffit et al., 2008; Raguso and Weiss, 2015). For example, floral volatile emissions often decline within minutes to hours of pollination (Muhlemann et al., 2006; Theis and Raguso, 2005), reflecting a down-regulation of volatile production by ethylene (Underwood et al., 2005) and a shift in allocation from floral display to fruit maturation, presumably to reduce both metabolic and ecological costs (Grison-Pigé et al., 2001; Janzen, 1981). Temporal variation of floral scent emission is widespread in nature (Matile and Altenburger, 1988) and is especially apparent, for example, in sphingophilous (night-blooming, hawkmoth pollinated) flowers. In such cases, the nocturnal scent emissions, which can be rhythmic in flowers lasting more than one evening, are synchronized with the activity period of the nocturnal pollinators (Hoballah et al., 2005; Kolosova et al., 2001), and often are weaker or qualitatively different during the day (Prieto-Benítez et al., 2015; Raguso et al., 2003). Further, individual volatiles within a blend may follow different temporal rhythms (Nielsen et al., 1995), lending additional complexity to the challenge of interpreting the multiple functions of floral scent. One plant that uses temporal variation in scent emission to manipulate pollinator behavior and thereby increase reproductive fitness is the Australian cycad species, *Macrozamia lucida* (Zamiaceae). These gymnosperms attract ("pull") their thrips pollinators (*Cycadothrips chadwickii*) to individuals bearing male cones and then repel ("push") those same pollinators to individuals bearing female cones by modulating the emission rates of common monoterpene volatiles (e.g. β-myrcene) and cone temperature

4

at different times of the day. A rhythmic increase in volatile emission, combined with a thermal blast, induces pollen-feeding thrips to leave male cones covered with pollen, after which they are attracted to female cones by the same volatiles at much lower emission rates, thus ensuring pollination by deceit (Terry et al., 2007; Terry et al., 2014).

Temporal variation of volatile emission is also expected in flowers or inflorescences when male and female functions are separated temporally (dichogamy) rather than spatially. This is especially relevant in protogynous kettle trap flowers (e.g. *Ceropegia*, Apocynaceae) or inflorescences (e.g. *Arum*, Araceae) that utilize elaborate morphological, tactile, visual and chemical aspects to attract and trap their pollinators (Heiduk et al., 2015; Ollerton et al., 2009; Renner, 2006; Urru et al., 2011). Additionally, the morphological features of trap flowers can be subdivided into distinct spatial zones, for example, within vs. outside of the trapping chamber. The structural independence of such floral features suggests the possibility of concerted spatio-temporal patterns of volatile emission that could optimize plant reproductive fitness through highly choreographed pollinator manipulation (Angioy et al., 2003).

Kettle trap flowers are thought to have first evolved in the basal angiosperm genus *Aristolochia* (Aristolochiaceae) (Oelschlägel et al., 2009), which includes some of the world's largest flowers (Davis et al., 2008) and most unusual floral scent blends (Oelschlägel et al., 2015). *Aristolochia* is a diverse genus consisting of roughly 450 species of vines, lianas, shrubs, or herbs with a predominately pantropical (but also warm-temperate) distribution (Endress, 1994; Judd et al., 2009; Wagner et al., 2014). Scent-mediated pollinator attraction and imprisonment in the protogynous kettle trap flowers of *Aristolochia* occur on the first day of anthesis, during the female phase of the

5

flower (Fig. 1) (Proctor et al., 1996). Visitors to *Aristolochia* flowers either are detained or simply remain within the floral chamber, and are showered with pollen when the flower transitions to the male phase, after which they depart as the flower senesces (Cammerloher, 1923; Costa and Hime, 1983; Gonzalez and Stevenson, 2000). Although *Aristolochia* flowers vary in size and morphology, the floral *bauplan* remains relatively constant throughout the genus. One of the largest-flowered species in the genus is *A. gigantea*, a liana native to tropical northeastern Brazil, especially in Bahia and Minas Gerais (Capellari-Junior, 1991; Costa & Hime, 1981). Flowers of *A. gigantea* are zygomorphic and consist of three congenitally united sepals that form a distinctive tube-shaped perianth that expands basally into a hollow trapping chamber (utricle) (Cammerloher, 1923; Correns, 1891; Costa and Hime, 1983; Gonzalez and Stevenson, 2000). Above the utricle, a narrow floral tube leads to a constricted opening, from which extends a conspicuous laminar surface (limb) with a calico-patterned visual display resembling the appearance of rotting flesh (Fig. 2A, B). Within the trap, six stamens are entirely adnate to a syncarpous style forming a gynostemium that is positioned above an inferior ovary (Gonzalez and Stevenson, 2000). Furthermore, the utricle contains two patches of glandular trichomes that secrete nectar on the first day of anthesis and become dark and visually conspicuous on the second day (Hipólito et al., 2012). The flowers are strongly protogynous with the gynoecium mature at anthesis (Hipólito et al., 2012), or sooner (own observations). Transition to the male phase occurs a day later, followed by a pronounced senescence beginning as soon as the third day of anthesis (own observations).

To the human nose, the character bearing note of the floral scent of *A. gigantea* is surprisingly pleasant, considering the fetid stench one might expect to accompany the flowers' meat-like visual display, as has been observed for *A. grandiflora* (Burgess et al., 2004) and *A. gorgona* (Blanco 2002). Instead of carrion, female stage flowers have an intense citronella scent. This observation is paradoxical given that the main floral visitors are phorid flies of the genus *Megaselia* (Phoridae; Diptera) (Hipólito et al., 2012), many of which utilize decaying organic matter (including senesced *Aristolochia* flowers) as brood sites (Disney and Sakai, 2001; Sakai, 2002). Thus, one might expect a brood-site deceptive flower pollinated by *Megaselia* flies to smell of decaying vegetation, as was described for *Aristolochia argentina* (Trujillo and Sérsic, 2006), rather than of sweet lemon. However, human perception can be misleading in chemical ecology, as mint and mustard compounds acceptable to the human palate can be deadly to insects (Isman, 2000), and biologically active volatiles are not always those that are most strongly emitted from flowers (Milet-Pinheiro et al., 2013). Thus, the powerful citronella scent of *A. gigantea* may mask more dilute but biologically active floral volatiles. Such compounds might include the oligosulfides (e.g. dimethyl trisulfide) characteristic of carrion-mimicry (Jürgens et al., 2013), indole and cresols present in fecal-mimicry (Jürgens et al., 2006; Urru et al., 2011), or the short-chain alcohols, ketones and esters indicative of yeast/fermentation mimicry (Goodrich and Raguso, 2009).

In this study we used chemical analysis to analyze the full suite of volatile compounds emitted by the distinctive kettle trap flowers of *Aristolochia gigantea* and to test for spatial and temporal differences in volatile production in this Neotropical pipevine. Specifically, we aimed to determine whether volatile compounds typical of

7

carrion, feces or rotting fruit/sap are emitted by the flowers of *A. gigantea*, but simply are not perceived by the human nose due to the masking effect of citronella-scent. Building on prior studies of similar trap flowers (Hadacek and Weber, 2002; Kite, 1995), we tested whether volatiles emitted by the flesh-like limb of *A. gigantea* differ in composition from those produced within the utricle, and whether volatile chemical patterns shift or even cease as flowers progressed from female to male phase (Stensmyr et al. 2002). Our studies revealed high chemical complexity and diversity of scent composition in flowers of *A. gigantea* across most biosynthetic classes, which changes markedly during floral ontogeny and between flower parts. These results suggest several avenues for further study, including behavioral assays and phylogenetic/comparative initiatives.

2. Materials and Methods

2.1 Plant Material

Aristolochia gigantea flowers used for volatile collection were obtained from a single large individual liana cultivated in the president's greenhouse of the University of South Carolina, Columbia, SC, USA. No information was available concerning the provenance of this plant, but it was identified to species by Mario Blanco (Univ. de Costa Rica). Pressed vouchers were deposited at the A.C. Moore Herbarium, University of South Carolina (USCH). The plant was watered and fertilized *ad libitum* and flowers were taken for analyses as they bloomed sequentially from March to early June in 2004 and 2005. The plant was grown in a glasshouse under natural lighting, as the glass panes were not whitewashed. Additional plants were studied at the Jardin Botanique de Montréal,

8

Canada by JH in 2011. These included *A. gigantea* (accession number 2097-1997), with flowers whose meat-like limb is extended into two dangling lobes, with an overall average limb length of 33 cm (some exceeding 50 cm), and *A. gigantea* (accession number 1461-2000), whose floral limbs lack the wattle-like extensions and thus are obovoid in shape (average limb length of 12 cm), similar to the plant studied in South Carolina. Finally, we used an additional, lobe-limbed individual of *A. gigantea* cultivated by Paul Cooper at Cornell University to verify certain volatile compounds and their mass spectra.

2.2 Volatile Collection

To test for spatial and temporal variation in volatile production, *A. gigantea* flowers of each distinct ontogenic stage (female, male, wilted; mean $\pm$ sem fresh mass over all stages = 12.779 $\pm$ 1.164 g) were dissected into individual functional units (limb [4.285 $\pm$ 0.439 g], black ring [0.757 $\pm$ 0.106 g], yellow disk (entrance to floral tube; 1.320 $\pm$ 0.090 g) and utricle = floral chamber [3.711 $\pm$ 0.254 g]; N = 9-15 replicates of each dissected flower part; see Fig. 2C) and subjected to volatile collection in parallel. In addition, we tested whether two patches of glandular trichomes (nectaries) within the utricle also might function as osmophores by dissecting them from the utricle (mean $\pm$ sem fresh mass 0.617 $\pm$ 0.050 g), along with a slightly larger section of the opposite wall of the chamber (0.808 $\pm$ 0.107 g) (about 21% total mass of the utricle), and collecting volatiles from them as described below. Fresh masses were obtained for most individual treatments immediately after volatile collection.

9

In addition, volatiles were collected from whole (entire) cut flowers at each stage, as well as from whole cut buds one day prior to anthesis, with cut pedicels excluded from the headspace bag. Volatiles were collected from 2-7 replicates of each age-flower part combination from the South Carolina plant in 2004 and 2005. Freshly cut entire flowers as well as dissected floral parts were placed within individual nylon resin oven bags (Reynolds Consumer Products, Lake Forest, IL) for 30 minutes to allow floral volatiles to equilibrate prior to collection. Headspace bags were prepared by cutting and resealing oven bags to standardized dimensions for whole flowers (15 x 15 cm) and dissected flower parts (11 x 11 cm) using an impulse heat sealer (American International Electric, Inc., City of Industry, CA). Following a 30 minute equilibration of each sample, a solid phase micro-extraction (SPME) fiber coated with polydimethylsiloxane and divinylbenzene (PDMS/DVD, 65µm film thickness, Supelco, Bellefonte, PA) was introduced to the equilibrated headspace and exposed for an additional 30 minutes, followed by immediate gas chromatography-mass spectrometry (GC-MS) analysis. These methods are sufficient to capture a broad spectrum of volatiles, including N- and S-bearing compounds likely to be present in brood-site deceptive flowers (Goodrich and Raguso, 2009). Vegetative and ambient controls were collected and subtracted from the floral volatile samples to identify volatiles unique to floral tissues. Peaks associated with the vegetative background were not integrated if they did not meet our criteria (3X that of the vegetative GC-MS peak areas) for designation as flower-emitted. Wound volatiles associated with the dissection of floral tissues were identified by comparing the chromatograms of cut vs. intact floral tissues, and were subtracted from the actual experimental replicates.

10

2.3 GC-MS Analysis

SPME samples were thermally desorbed at 240°C in the injection port of a Shimadzu

GC-17A gas chromatograph coupled with a Shimadzu QP5000 electron impact

quadrupole mass spectrometer used as a detector. Directly after desorption, volatiles were

injected in splitless mode onto a polar polyethylene glycol GC column (30m length,

0.25mm ID, 0.25µm film thickness, EC^{TM} Wax, Grace, Deerfield, IL) using helium as a

carrier gas with a flow rate of 1.2ml min^{-1}. Oven temperature was held at 40°C for 3

minutes, then ramped at 10°C min^{-1} to 260°C and held for 5 minutes. Mass spectra were

obtained using an ionization energy of 70 eV and an interval of 0.29 seconds.

Chromatographic peaks were integrated using Shimadzu GCMSsolution software (v.

4.20) and were tentatively identified using NIST, Wiley, and Adams mass spectral

libraries (see Schlumpberger and Raguso, 2008). When possible, peak identity was

confirmed using authentic standards. When standards were not available, the Kovats

Retention Index of each peak was calculated and compared to published values by

consulting databases such as Pherobase

(http://www.pherobase.com/database/kovats/kovats-index.php) and Flavornet

(http://www.flavornet.org/flavornet.html), as well as the primary literature (see Friberg et

al., 2013). When neither authentic standards nor published Kovats Indices were available,

the tentative mass spectral library identification was listed as a place holder for that

compound when the matching strength was 90% or greater. If none of these requirements

were satisfied, the peak identity was classified as "unknown" and listed with the ten most

abundant mass spectral ion fragments in ascending order of m/z.

11

Volatile compounds were assigned to categories following Knudsen et al. (2006), including aromatic compounds (containing a benzene ring), aliphatic compounds (linear or branched compounds lacking aromatic rings), terpenoids (C_{10} [monoterpenoids] or C_{15} [sesquiterpenoids] isoprene-derived compounds which may be oxygenated), N- and S-bearing compounds. Compounds whose mass spectra were not distinctive enough to allow assignment were categorized as "unknown". The aliphatic category includes products of very different biosynthetic pathways with distinctive chemical ecological functions, such as the linolenic acid derived C6 and C8 alcohols and esters associated with wounding, collectively known as the "green leaf volatiles" (Matsui, 2006). When possible, compounds from sub-categories such as this were grouped beneath the major headings of chemical classification (see Table 1). Contrary to Knudsen et al (2006), we have included C5 branched compounds derived from LEU and ILE among the aliphatics, in recognition that aliphatic compounds are not a natural group, and that the classification scheme of Knudsen et al. (2006) largely reflects structure, not biosynthetic origin.

2.4 Multivariate Analyses

The total ion chromatogram peak areas for each floral volatile compound were converted into presence/absence values (1 if present, 0 if absent). Reduction to presence/absence values can be considered the end point of ever-increasing power transformations (Clarke and Gorley, 2006), and was used to give equal weight to each compound present in a sample based on our non-quantitative volatile sampling procedures (SPME-GC-MS, non-standardized floral masses). Presence/absence data were then used to visualize spatio-temporal changes in floral scent using multidimensional scaling (MDS) analysis in

PRIMER v6 (Clarke and Gorley, 2006). Briefly, presence/absence data were used to calculate a similarity matrix using the Sørensen similarity index (the qualitative equivalent to the Bray-Curtis similarity index) as described by Majetic et al. (2014). A two-way crossed analysis of similarity (ANOSIM) was then used to examine differences between flower stages and between flower parts, using 10,000 permutations to calculate global R-values to assess the similarity between each pairwise comparison, with larger global R-values (ranging from 0-1) accompanied by significant p-values indicating high dissimilarity (Clarke, 1993; Clarke and Gorley, 2006). To assess similarities between each stage-part sample type (e.g. female chamber vs. male limb, etc.) a one-way ANOSIM was calculated by combining stage and part into a single factor (stage x part) and using the same statistical criteria as above. When ANOSIM indicated significant differences between stage-parts we conducted a similarity percentage test (SIMPER) to explore how each volatile contributed to the overall differences (see Arguello et al., 2013). Because SIMPER analyses are less meaningful when based on presence/absence data (all contributions to dissimilarity are equal) we applied a less stringent but still conservative data transformation by calculating the relative abundance of each compound with respect to the total peak area within each sample, and then applying a square root transformation to each standardized value. This allowed us to explore the ranked percentage of likely volatile contributions to the dissimilarity of sample groups while still restricting the effect of highly abundant compounds in each sample.

3. Results

3.1 Chemical Composition

The floral scent of *Aristolochia gigantea* is strikingly complex. SPME-GC-MS analyses revealed a total of 168 volatile compounds, belonging to diverse chemical classes, across all floral organs and ontogenic stages (Table 1). We identified 28 uniquely floral monoterpene (C_{10}) hydrocarbons, alcohols, aldehydes and acetates, along with a similar number of flower-specific sesquiterpene (C_{15})-related compounds. The floral scent of *A. gigantea* also includes a large number (40) of aliphatic ketones (with related alcohols and aldehydes), especially a series of 2-ketones emitted largely on the first day of anthesis. We identified 27 fatty acid- and amino-acid derived aliphatic compounds, 6 of which are alcohols or esters with a 3-methyl-1-butanol moiety, along with related alcohols and ketones. Twelve compounds could be unequivocally categorized as alkanes or alkenes, with another 19 unknowns that could not be identified or assigned to class. Finally, flowers of *A. gigantea* emit 9 aromatic compounds (e.g. anisole, benzyl alcohol), three of which are esters of 3-methyl-1-butanol, along with one sulfur-bearing compound (dimethyl disulfide) and no nitrogen-bearing compounds. Flowers emitted additional terpenoid compounds shared with vegetative tissues, which were omitted from further analysis as non-floral background chemistry, due to similar volatile profiles between immature flower buds and leaves (not shown). Similarly, several green-leaf volatiles (e.g. hexyl acetate, (*Z*)-3-hexen-1-ol) detected from dissected flower parts were omitted from further analysis as artifacts of wounding.

3.2 Temporal Patterns of Scent Emission

Strong differences in volatile composition were observed between different reproductive stages of the protogynous flowers of *A. gigantea* during their development (Figs. 3A, C),

both in the number and diversity of volatile compounds produced (ANOSIM global $R =$ 0.979, p = 0.004), as well as in the total amount of scent emitted. Female stage flowers emit the most intense and chemically diverse volatile blends, with a total of 137 compounds across all floral parts (Fig. 3). Female stage whole flowers are characterized by the simultaneous emission of 2-heptanone, dimethyl disulfide, 3-methyl-1-butanol and its associated acetate, along with potent amounts of lemon-scented terpenoids, including citronellal, (*Z*)-citral (neral), (*E*)-citral (geranial), citronellol, nerol, and geraniol (Table 1).

Floral scent changes dramatically as flowers enter the male phase of development, usually one day after opening. Volatile emission is highly reduced (resulting in 78 total compounds across all floral parts), represented both by diminished emissions of compounds present in the female stage and also by the emission of novel volatiles (Figs. 3A, B; Table 1). Male stage whole flowers transition to the production of novel and intense emissions of linalool, (*Z,E*)-α-farnesene and (*E,E*)-α-farnesene and their oxygenated derivatives (Table 1). The ontogenic reduction of volatile emission continues in wilted (senescent) flowers (resulting in 43 total compounds across all floral parts), which chemically resemble the vegetative background (Fig. 3A, B; Table 1). Wilted flowers continued to produce 3-methyl-1-butanol and anisole (found in all floral stages), but ceased to produce β-myrcene and (*E*)-β-ocimene present in greater quantity in female and male stage flowers (Table 1). Whole flower analyses of *A. gigantea* from the Jardin Botanique de Montréal and from Cornell University revealed the same major patterns, with MS detector-saturating amounts of citrals and related terpenoids emitted by first day

15

flowers and noteworthy peaks of linalool, farnesenes and related compounds emitted by second day flowers (data not shown).

3.3 Spatial Patterns of Scent Emission

Spatial patterns of scent composition differed markedly within and between sexual stages (Figs. 3C, S1, 2; Table S1) (two way ANOSIM, flower parts; global $R = 0.607$, p = 0.001; flower stages; global $R = 0.774$, p = 0.001). For clarity of presentation, we discuss spatial patterns in two inclusive categories; external flower parts visible to approaching insects (limb, black ring, and yellow disk of the floral tube), and internal parts that would be apparent to trapped visitors (utricle and nectaries).

3.3.1 External Floral Parts

The large, meat-like floral limb emits 87 volatiles during female phase, including massive amounts of citrals and complex blends of ketones and alcohols, but is essentially scentless in male and wilted phases, emitting only small amounts of 12-13 compounds respectively (ANOSIM global R = 0.742, p = 0.003; Fig. 4A, B; Table 1). Consistent amounts (peak areas) of 3-methyl-1-butanol and anisole are emitted from the limb throughout each flower's lifetime, whereas the relative percentages of these compounds increase (as statistical artifacts) as other volatiles cease. 103 volatile compounds were identified from the velvet-black ring of the limb during female phase, dominated by a series of 2-ketones (2-pentanone through 2-tridecanone) along with some branched ketones and alcohols, many of which are specific to this tissue and ontogenic stage and are seldom emitted from male or senescent flowers (Table 1). Similarly, the conspicuous

16

yellow disk of the open floral tube emits 52 volatiles during female phase but only 14 compounds in male and wilted phases, degrading from a complex blend of ketones, alcohols and 3-methylbutyl esters to a simple blend of compounds common to the male phase utricle, such as linalool (see section 3.3.2 below).

3.3.2 Internal Floral Parts

The contrast between female and male stage volatile emissions from the utricle was the most surprising result of this study (ANOSIM global R = 0.521, p = 0.002). Dimethyl disulfide is emitted by female stage flowers only, with the greatest amount emitted from the chamber and the black ring of the limb surrounding the entrance to the floral tube, but is absent from the lobed, calico patterned portion of the limb resembling rotting flesh. Quantitatively, the scent of female-stage chambers is dominated by large peaks of 3-methylbutyl 3-methylbutanoate, benzyl methyl ether, β-myrcene and (*E*)-β-ocimene, along with several alkanes and terpene hydrocarbons (e.g. limonene, (*E*)-β-caryophyllene) common to the foliage of *A. gigantea.* By day 2, when anthers are dehiscing and the stigmatic surface is senescing within the utricle, there is a nearly complete turnover in volatile composition within this chamber, with large amounts of linalool, methyl geranate, (*Z,E*) and (*E,E*)-α-farnesene emitted in place of the compounds listed above (Figs. 4C, D; Table 1). Follow-up assays revealed that the major acyclic terpenoids are produced in disproportionately large amounts by the twin patches of nectar-secreting tissue within the utricle.

4. Discussion

4.1 The multidimensional floral scent of *Aristolochia gigantea*

Based on morphological characters alone (Fig. 2), one might expect the impressively meat-like flowers of *Aristolochia gigantea* to be pollinated by saprophytic flies and to emit a nauseating carrion-like stench (Burgess et al., 2004; Proctor et al., 1996). Indeed, we detected small amounts of dimethyl disulfide (Table 1, Fig. 4C), which, along with dimethyl trisulfide, is indicative of carrion mimicry in brood-site deceptive flowers worldwide (Jürgens et al., 2013). However, in such cases volatile sulfides are the dominant components of simple scent bouquets (Jürgens et al., 2006; Kite and Hetterscheid, 1997; Stensmyr et al., 2002) that attract calliphorid, sarcophagid and muscid flies (Moré et al., 2013; van der Niet et al, 2011; Shuttleworth and Johnson, 2010). The complex pattern of floral volatiles emitted by *A. gigantea* departs markedly from the simple expectations of carrion mimicry. Dimethyl disulfide is not emitted by the large, meat-like limb, but instead by the utricle (floral chamber) and the bright yellow disk of the floral tube leading to it during the first day of anthesis, when the stigmatic lobes of the gynostemium are receptive (Table 1, Fig. 4C). Conversely, the meat-like limb emits lemon-scented, oxygenated monoterpenes during the same period, in amounts that saturated our MS detector (Fig. 4A), on a schedule that coincides with the arrival of pollen-bearing phorid flies to these flowers (Costa and Hime, 1981, Hipólito et al., 2012). This interplay between floral morphology and scent constitutes a botanical paradox, as the visually contrasting lemon-like disk (Fig. 2A, C) leading to the chamber smells of rotting meat and decaying fruit, whereas the meat-like limb (Figs. 1, 2) emits a lemon-scented plume powerful enough to attract visitors from a distance.

18

Stefan Vogel's (Vogel, 1963; English translation, 1990) landmark study of osmophores - the floral tissues responsible for biosynthesis and release of volatiles - was published before capillary GC-MS was first used to analyze floral scent. Vogel discussed the anatomy and histology of *Aristolochia* aff. c*ordiflora*, which closely resembles *A. gigantea* (1990; his Fig. 11, p. 37). (Note, given the absence of a yellow disk in *A. cordiflora* and the absence of vouchers from Vogel's study at Mainz, we infer that his plant likely was *A. gigantea*). He was struck by the similarities in floral *bauplan* between these taxa but was misled by the descriptions of Hoene (1942), who attributed an unpleasant scent to flowers of *A. gigantea* cultivated in the Jardim Botânico, Rio de Janeiro, an observation that was disputed by Costa and Hime (1981) in subsequent studies at the same location. Vogel also was surprised by the strong, non-fetid quality of this flower's scent, which he compared to Melissa oil (*Melissa officinalis* = lemon balm), an essential oil dominated by citrals and citronellal (Shabby et al. 1995). Initially, he suggested that the conspicuous yellow disk of the floral tube was the primary source of volatiles, due to its glandular surface, high starch content and weak thermogenic properties, and his observation that the starch granules within this tissue were exhausted (along with scent and heat) by the second day of anthesis. However, further investigation convinced Vogel "that the thin limb [is] likewise odoriferous". Despite Vogel's conjecture, based on his careful anatomical study of the yellow disk, our SPME-GC-MS analyses show that lemon-scented monoterpenoids are emitted exclusively from the floral limb of *A. gigantea* (Fig. 4, Table 1). The yellow disk emits a diverse mix of non-terpenoid volatiles, some of which are shared with (and may adsorb passively from) the

19

utricle (Table 1). However, the yellow disk is adnate to the velvet-like black ring of the limb, which is the richest source of floral volatiles in *A. gigantea*. The complex vascular network diagrammed by Vogel (1990; his Fig. 12 II, p. 40) within the yellow disk may communicate with the adjacent ring and thus mediate volatile translocation and secretion.

Having determined the chemical identity, timing and source of the strong citronella scent emitted by flowers of *A. gigantea* (Fig. 4, Table 1), we have yet to discover its function. The smell of citronella often is associated with repellent properties for flies and mosquitoes (EPA, 1999; Fradin and Day, 2002), and it is possible that the citral plume emitted by the limb of *A. gigantea* is a floral filter that prevents deleterious insects from entering the floral chamber (Shuttleworth and Johnson, 2009). Other pollinator groups may be attracted to citronella, including bees (Faria and Stehmann, 2010; Pearson and Dressler, 1985) and non-saprotrophic flies (Howlett, 1912), but available data do not support this hypothesis (Costa and Hime, 1981; Hipólito et al., 2012). Finally, Hadacek and Weber (2002) suggest that spatial scent gradients and chemical contrast may enhance pollinator capture in kettle trap flowers with complex scent blends (see section 4.3 below). In our system, phorid flies may be attracted from a distance by the visual and olfactory cues of lemons or similar fruit, but upon arrival at flowers of *A. gigantea*, are compelled by dimethyl disulfide and fermentation-related volatiles to enter the floral tube and chamber (Fig. 1), where they feed on nectar and pollen (Hipólito et al., 2012). "Bait and switch" floral advertisement has been described for *Epipactis helleborine* orchids, whose flowers attract caterpillar-hunting wasps with the scent of wounded leaves, then reward the wasps with nectar instead of protein (Brodmann et al., 2008). Depending on the precise time at which the chamber scent of *A.*

20

gigantea shifts from carrion/fermentation volatiles to sweet floral emissions (linalool, ocimenes, farnesenes; Fig. 4C, D), the shift in scent may either encourage phorid flies to feed (pull) or, alternatively, may compel them to leave the utricle (push), seeking other flowers.

4.2 Insights from Phorid Fly Pollinators

Our speculation on the possible behavioral importance of spatio-temporal orchestration of volatile release in flowers of *A. gigantea* underscores the importance of making field observations of native floral visitors to wild plants. Hipólito et al. (2012) studied natural, blooming populations of *A. gigantea* in Chapada Diamantina, Bahia, Brazil, and noted the same powerful citronella floral scent that we document here. The primary pollen-carrying insects found within the floral chambers of *A. gigantea* were several morpho-species of scuttle flies (family Phoridae) in the genera *Pseudohypocera* and *Megaselia*, which arrived at newly opened flowers between 06:30 and 08:00 hrs, coincident with the onset of scent emission. Flies directly approached the yellow disk, landed at the mouth of the floral tube and entered the utricle. Flies remained within the utricle during the female phase, feeding on the secretions of twin patches of glandular trichomes on the chamber wall and from the stigmatic lobes of the gynostemium (Costa and Hime, 1981). These secretions qualify as true nectar, dominated by sucrose (56-69%) with smaller percentages of fructose (20-30%) and glucose (12-14%) (Hipólito et al., 2012) as well as amino acids (Costa and Hime, 1981). Phorid flies moved throughout the utricle during the first day seeking nectar and remained within the flowers even though the trichomes of the floral tube did not hinder their departure (Hipólito et al., 2012). By the following

21

morning (male phase), nectar is no longer secreted by the (now darkened) nectaries, and floral scent has shifted perceptibly. Video recordings indicate that flies remaining in the utricle at this point move to the gynostemium and feed on pollen before exiting through the floral tube carrying pollen, and then taking flight from the black ring (Hipólito et al., 2012). Based on their frequency as visitors, the pollen masses attached to their bodies and the quantity of pollen tubes associated with flowers they have visited, Hipólito et al. (2012) considered *Megaselia* spp. to be the primary pollinator of *A. gigantea* in the Chapada Diamantina. *Pseudohypocera* spp, flies also were found with pollen grains attached to their bodies, but were less abundant at the study localities. Females outnumbered males by a roughly 5:1 ratio for both species. Costa and Hime (1981) identified a similar assemblage of floral visitors to cultivated *A, gigantea* plants in Rio de Janeiro, dominated by *Pseudohypocera kerteszi* (91% of all visits). The only pollen type carried by this species belonged to *A. gigantea*, suggesting that these flies do not visit other flowers locally. Costa and Hime (1981) observed pollen deposition on the mesonotum of *P. kerteszi* flies, where setae facilitate its accumulation until the flies are cloaked with pollen. *Pseudohypocera kerteszi* flies are distributed across tropical America, where they are major kleptoparasites of meliponine (stingless bee) hives, in which their larvae develop by consuming brood resources (pollen, nectar, nest materials; Robroek et al., 2003a). However, only adult female *P. kerteszi* flies are observed to enter the hives of their meliponine bee hosts (Robroek et al., 2003b), whereas nearly all (96%) of the *P. kerteszi* flies observed by Costa and Hime (1981) to visit flowers of *A. gigantea* were male. Thus, the floral volatiles of *A. gigantea* are more likely to mimic sexual

attraction of male *P. kerteszi* than brood-site cues that attract female flies to stingless bee hives.

Sex-specific attraction is a common theme in fly-pollinated *Aristolochia* species. *Megaselia* flies also pollinate other species of *Aristolochia,* including *A. inflata* in Panama (Sakai 2002) and *A. argentina* in Argentina (Trujillo and Sérsic, 2006), whose floral scents evoke organic decay to human sensibilities, but have not yet been chemically analyzed. All visitors to *A. inflata* and *A. argentina* were females. In contrast, males accounted for 334 of 349 visitors (mostly *Megaselia scalaris, M. aurea* and *M. perdita*) to 32 flowers of the Brazilian species *A. littoralis* (= *elegans*) naturalized in Florida, USA (Hall and Brown, 1993). Similarly, all individuals of three pollen-carrying *Megaselia* morpho-species visiting *A. pallida* in Italy were male (Rulik et al., 2008). Clearly, further insights on the floral evolution of many Neotropical *Aristolochia* species will require a deeper understanding of the chemical and reproductive ecology of *Megaselia* flies, whose 1500 described species represent a small fraction of actual phorid diversity (Disney, 1994). *Megaselia* flies are thought of as generalized scavengers, probably due to the ubiquitous and polyphagous *Megaselia scalaris* (Loew), which is frequently used in forensic studies (Disney, 2008). Nevertheless, there are many examples of extremely specialized larval hosts in this genus, from frog eggs to the hyphae of fungi developing within adult pentatomid bugs (Brown and Horan, 2012; Ceryngier et al., 2006). Interestingly, larvae from several *Megaselia* species feed exclusively on flowers of *Aristolochia* species (Disney and Sakai, 2001), some of which (e.g. *A. inflata*) appear to have evolved a nursery pollination mutualism (Sakai, 2002).

4.3 Variations on a Floral Trap

23

One advantage to studying species-rich lineages of flowering plants is the opportunity to explore the diversification of specific floral niche dimensions (Johnson, 2010) and their repeated evolution (Castellanos et al., 2004). With at least 450 species, a pan-tropical distribution and an unusual floral *bauplan* conducive to trap-and-release pollination systems, the genus *Aristolochia* provides rich opportunities to study floral niches poorly represented in the post-glacial temperate environments that have dominated the study of pollination (Johnson and Steiner, 2000). The extensive literature on *Aristolochia* reveals strong associations with different lineages of Diptera, including several species pollinated by the Phoridae, as discussed in section 4.2 above. Additional pollinator niches in *Aristolochia* include Anthomyiidae and Chloropidae (*Elachiptera* sp., all males) in Russian *A. manshuriensis* (Nakonechnaya et al., 2008), Drosophilidae in Panamanian *A. maxima* (Sakai, 2002), Chironomidae in Indian *A. tagala* (Murugan et al., 2006), Ceratopogonidae (*Foripomya* sp.) in Pakistani *A. bracteolata* (Razzak et al., 1992) and Sri Lankan *A. indica* (Petch, 1924), and female Chloropidae and Milichiidae in Panamanian *A. pilosa* (Wolda & Sabrosky, 1986). Chemical analyses, combined with behavioral assays (see Hall and Brown, 1993) performed on any of these species would likely reveal fundamental aspects of brood-site, mate location, or food location by members of these fly lineages. Central American *A. grandiflora* is a classic example of carrion mimicry, with immense, fetid trap flowers that lack nectaries (Cammerloher, 1923; Hilje, 1984). Interestingly, *A. grandiflora* successfully recreates the niche of rotting flesh, as it not only attracts calliphorid flies as pollinators, but also elicits oviposition by hundreds of non-pollinating phorid flies and similar numbers of staphylinid beetles that prey upon their larvae (Burgess et al., 2004). In a bizarre twist on fly pollination, flowers

24

of the European *A. rotunda* specifically attract chloropid flies with a chemical blend

(hexyl esters and short chain alkanes) that mimics the wound volatiles emitted by

recently killed mirid bugs (Hemiptera). These kleptoparasitic flies (*Trachysiphonella*

ruficeps) steal food from other insects, and in this case specifically imbibe the secretions

from mirid bugs killed by other arthropods (Oelschlägel et al., 2015). Finally, the larger

Aristolochiaceae, which now includes the former Piperaceae, Saururaceae and

Hydnoraceae (APG, 2016), includes additional pollinator niches, including fungal

mimicry in the ground-blooming genus *Asarum* and the cauliflorous *Aristolochia arborea*

(Kaiser, 2006; Sinn et al., 2015; Vogel, 1978). The fetid, fleshy flowers of *Hydnora*

africana, a root parasitic species, emit sulfur volatiles (Burger et al., 1988) and form

subterranean chambers that trap tenebrionid beetles in southern Africa, suggesting a

rotting-hide niche (Bolin et al., 2009).

It is intriguing to consider that each of the niches described above for *Aristolochia*

(and others yet to be documented) have arisen through convergent evolution in other

lineages with kettle trap flowers (Renner, 2006). Despite the elaborate morphology of

Aristolochia flowers, kettle trap floral plans are not unique to this genus. Flowers of

Ceropegia (Apocynaceae, Asclepiadoideae) and inflorescences of *Arum* (Araceae) show

strikingly similar floral ground plans including sophisticated trapping mechanisms that

are enhanced by dichogamous maturation of the fertile organs (Gibernau et al., 2004;

Masinde, 2004; Ollerton et al., 2009). Remarkably, in each of the respective genera, the

trap is formed by the modification of a different floral or sometimes vegetative tissue. For

example, the genus *Aristolochia* utilizes the first floral whorl, i.e. a congenitally united

calyx to form the trapping chamber. In contrast, *Ceropegia* achieves the same structure

25

by congenital fusion and basal inflation of the corolla (Ollerton et al., 2009), while the genus *Arum* and related plants forgo floral tissues altogether and enclose their male and female florets within a highly modified bract (Bröderbauer et al., 2012; Meeuse and Raskin, 1988). As recognized by Vogel (1990), whose treatise on osmophores featured many examples from these lineages, floral scent can be highly chemically diverse among *Ceropegia, Arum, Amorphophallus* and other aroid lineages, including chemically mediated mimicry of carrion, herbivore and carnivore feces and rotting fruit/yeast (Kite et al., 1998; Stökl et al., 2010; Urru et al., 2011). One remarkable parallel to the niche described above for *Aristolochia rotunda* (pollination by kleptoparasitic flies) was described recently for *Ceropegia dolichophylla*, to which volatile spiroacetals attract Milichiid fly pollinators that, under normal circumstances, feed from the secretions of wounded arthropods (Heiduk et al., 2010).

Our study of *Aristolochia gigantea* was inspired, in large part, by Hadacek and Weber's (2002) detailed chemical analysis of floral scent in *Sauromatum guttatum*, an aroid that has served as a model system for the study of thermogenesis in plants (Meeuse, 1975; Raskin et al., 1989). Although a range of chemical methods had been used to document scent composition in *S. guttatum* (Borg-Karlson et al., 1994; Skubatz et al., 1996; Smith and Meeuse, 1966), Hadacek and Weber (2002) used SPME-GC-MS to provide the first glimpse at unexpected chemical complexity (over 200 identified volatiles) and spatial variation in scent blends emitted along the length of the sterile spadix and by the florets and club shaped organs enclosed within the spathe. These authors speculated that the strong lemon scent (β-citronellene) emitted by the distal end of the appendix provides chemical contrast with fetid volatiles within the trap, making it

easier for fly pollinators to locate the reproductive organs. A similar hypothesis could be advanced for *A. gigantea*, whose flowers smell like lemon on the outside and emit dimethyl disulfide and fermentation-related volatiles from the utricle and its entrance. This discussion underscores an important feature of kettle trap flowers: pollinators must be induced to enter them, either through visual contrast, chemical gradients, tactile cues and/or heat (Angioy et al., 2004; Diaz and Kite, 2006). This holds true for other pollinator niche dimensions in kettle trap flowers, in which strong fragrances and thermogenesis attract scarab beetles to *Philodendron* and related aroids as rendezvous sites (Dötterl et al., 2012; Gottsberger and Silberbauer-Gottsberger, 1991).

4.4 Caveats and New Horizons

We are well aware that the primary data set for this study is pseudoreplicated, as data were collected from multiple flowers on the same cultivated plant over two consecutive years. Our use of multivariate methods is entirely illustrative, rather than for strict hypothesis testing (Figs. 3C, S1, 2, 3). Unlike Hipólito et al. (2012), our primary goal was not to assess population level variation in nature, but to utilize a cultivated, mass blooming plant for in-depth chemical analyses in the tradition of Vogel's (1990) histological studies of cultivated plants. Our intensive sampling scheme would have been challenging to perform within the plant's native range (Chapada Diamantina, Bahia; Hipólito et al., 2012) or even in the Jardim Botânico, Rio de Janeiro (Costa and Hime, 1981). Given the stunning spatio-temporal variation in scent composition documented here, our sampling strategy was essential to generate confidence in the reproducibility of our data. Subsequent analyses from other individuals of *A. gigantea* cultivated in

Montreal, Canada and at Cornell University are highly consistent with the data presented here.

Another caveat is that the complex floral scent composition documented in Table 1 is best viewed as a conservative estimate, based on several methodological considerations. First, the use of GC-MS alone was not sufficient to confidently identify all compounds analyzed in this study, resulting in many mass spectra that are not identifiable without further analytical approaches. Second, floral scent of *A. gigantea* includes related series or "runs" of very similar compounds (e.g. sesquiterpene hydrocarbons) that ideally would require additional chromatographic dimensions to fully separate (Marriott and Shellie, 2002). The use of GCxGC-MS could easily double the number of compounds identified in samples as rich as these. Moreover, many of the volatile compounds identified in this study (e.g. linalool, citronellol) contain chiral centers and may exist in different enantiomers (Dötterl et al., 2006). Again, the incorporation of a chiral GC column into a multi-dimensional GC-MS analytical system (Begnaud et al., 2006) would be necessary to fully characterize the enantiomeric diversity of these samples.

Finally, in the absence of a definitive behavioral assay, we are left to speculate how such a highly coordinated, spatially and temporally dynamic display of volatile floral chemistry might manipulate pollinator behavior to the plant's reproductive advantage. Iterative chemical fractionation vetted with bioassays (e.g. Murphy and Feeny, 2006) is a core approach in the field of chemical ecology, with the desirable outcome of focusing chemical analysis on behaviorally active or ecologically important fractions of a natural blend (see Oelschlägel et al., 2015). In the absence of controlled

bioassays with *Megaselia* and other phorid flies, we cannot begin to prudently evaluate the behavioral roles of so many female stage volatiles. The growing literature on the pollination of *Aristolochia* highlights the importance of phorid flies to floral diversification in a lineage of ancient angiosperms, and reinforces how little we know about this diverse family of flies and the other flowers that they pollinate (Borba and Semir, 2001). The Phoridae are comparable in diversity to the Drosophilidae (fruit and fungus flies, c. 3000 spp) and the Sciaridae (fungus gnats, c. 1700 spp), two fly families whose members pollinate diverse lineages of Pleurothallid orchids (c. 4000 spp) in tropical America, such as *Lepanthes* (Blanco and Barboza, 2005) and *Dracula* (Policha et al., 2016). Integrated studies of floral chemistry and pollinator behavior promise to shed light on the origins and maintenance of such diversity.

References

Angioy, A.M., Stensmyr, M.C., Urru, I., Puliafito, M., Collu, I., Hansson, B.S., 2004. Function of the heater: the dead horse arum revisited. Proc. R. Soc. B. 271(Suppl 3), S13-S15.

APG The Angiosperm Phylogeny Group., 2016. An update of the Angiosperm Phylogeny Group classification for the orders and families of flowering plants: APG IV. Bot. J. Linn. Soc. 181(1), 1-20.

Arguello, J.R., Sellanes, C., Lou, Y.R., Raguso, R.A., 2013. Can yeast (*S. cerevisiae*) metabolic volatiles provide polymorphic signaling? PloS one. 8(8), e70219.

Begnaud, F., Starkenmann, C., Van de Waal, M., Chaintreau, A., 2006. Chiral multidimensional gas chromatography (MDGC) and chiral GC–olfactometry with a double-cool-strand interface: application to malodors. Chem. Biodivers. 3(2), 150-160.

Blanco, M.A., Barboza, G., 2005. Pseudocopulatory pollination in *Lepanthes* (Orchidaceae: Pleurothallidinae) by fungus gnats. Ann. Bot. 95(5), 763-772.

Bolin, J.F., Maass, E., Musselman, L.J., 2009. Pollination biology of *Hydnora africana* Thunb. (Hydnoraceae) in Namibia: Brood-site mimicry with insect imprisonment. Int. J. Plant Sci. 170(2), 157-163.

Borba, E.L., Semir, J., 2001. Pollinator specificity and convergence in fly-pollinated *Pleurothallis* (Orchidaceae) species: a multiple population approach. Ann. Bot. 88(1), 75-88.

Borg-Karlson, A.K., Englund, F.O., Unelius, C.R., 1994. Dimethyl oligosulphides, major volatiles released from *Sauromatum guttatum* and *Phallus impudicus*. Phytochemistry. 35(2), 321-323.

Bröderbauer, D., Diaz, A., Weber, A., 2012. Reconstructing the origin and elaboration of insect-trapping inflorescences in the Araceae. Am. J. Bot. 99(10), 1666-1679.

Brodmann, J., Twele, R., Francke, W., Hölzler, G., Zhang, Q.H., Ayasse, M., 2008. Orchids mimic green-leaf volatiles to attract prey-hunting wasps for pollination. Curr. Biol. 18(10), 740-744.

Brown, B.V., Horan, R.V., 2012. A key to Neotropical Region frog-egg-feeding species of *Megaselia* (Diptera: Phoridae), with a new species from Panama. Contrib. Sci. 520, 1-4.

Burger, B.V., Munro, Z.M., Visser, J.H., 1988. Determination of plant volatiles 1: Analysis of the insect-attracting allomone of the parasitic plant *Hydnora africana* using grob-habich activated charcoal traps. J. High Resolut. Chromatogr. 11(6), 496-499.

Burgess, K.S., Singfield, J., Melendez, V., Kevan, P.G., 2004. Pollination biology of *Aristolochia grandiflora* (Aristolochiaceae) in Veracruz, Mexico. Ann. Missouri Bot. Gard. 91(2), 346-356.

Cammerloher, H., 1923. Zur Biologie der Blüte von *Aristolochia grandiflora* Swartz. Plant Syst. Evol. 72(6), 180-198.

Capellari-Junior, L., 1991. Espécies de *Aristolochia* L. (Aristolochiaceae) ocorrentes no estado de São Paulo (Species of Aristolochia L.(Aristolochiaceae) in the State of São Paulo). Universidade Estadual de Campinas.

Castellanos, M.C., Wilson, P., Thomson, J.D., 2004. 'Anti-bee' and 'pro-bird' changes during the evolution of hummingbird pollination in *Penstemon* flowers. J. Evol. Biol. 17(4), 876-885.

Ceryngier, P., Durska, E., Disney, R.H.L., 2006. The surprising larval habits of *Megaselia minor* (Zetterstedt, 1848) (Diptera: Phoridae). Stud. Dipterol. 12, 357-361.

Clarke, K.R., 1993. Non-parametric multivariate analyses of changes in community structure. Aust. J. Ecol. 18(1), 117-143.

Clarke, K.R., Gorley, R.N., 2006. User manual/tutorial. Primer-E Ltd., Plymouth, UK.

Correns, C., 1891. Beiträge zur biologischen Anatomie der *Aristolochia*-Blüte. Jahrb. Wiss. Bot. 22, 161-189.

Costa, E.L., Hime, N.C., 1981. Biologia floral de *Aristolochia gigantea* Mart. & Zucc. (Aristolochiaceae). Rodriguésia. 56, 23-32.

Costa, E.L., Hime, N.C., 1983. Observacoes sobre a biologia floral de *Aristolochia macroura* Gomez (Aristolochiaceae). Atas Soc. Bot. Brasil Rio De Janeiro. 1(11), 63-66.

Davis, C.C., Endress, P.K., Baum, D.A., 2008. The evolution of floral gigantism. Curr. Opin. Plant Biol. 11(1), 49-57.

Diaz, A., Kite, G.C., 2006. Why be a rewarding trap? The evolution of floral rewards in *Arum* (Araceae), a genus characterized by saprophilous pollination systems. Biol. J. Linn. Soc. 88(2), 257-268.

Disney, R.H.L., 1994. Scuttle Flies: The Phoridae, first ed. London, UK.

Disney, R.H.L., 2008. Natural history of the scuttle fly, *Megaselia scalaris*. Annu. Rev. Entomol. 53, 39-60.

Disney, R.H.L., Sakai, S., 2001. Scuttle flies (Diptera: Phoridae) whose larvae develop in flowers of *Aristolochia* (Aristolochiaceae) in Panama. Eur. J. Entomol. 98(3), 367-374.

Dobson, H.E., 1994. Floral volatiles in insect biology, in: Bernays, E. (Ed.), Insect-Plant Interactions Volume V. CRC Press, Boca Raton, FL, pp. 47-81.

Dobson, H.E., Bergström, G., Groth, I., 1990. Differences in fragrance chemistry between flower parts of *Rosa rugosa* Thunb. (Rosaceae). Isr. J. Bot., 39(1-2), 143-156.

Dobson, H.E., Groth, I., Bergstrom, G., 1996. Pollen advertisement: chemical contrasts between whole-flower and pollen odors. Am. J. Bot. 83(7) 877-885.

Dötterl, S., Burkhardt, D., Weißbecker, B., Jürgens, A., Schütz, S., Mosandl, A., 2006. Linalool and lilac aldehyde/alcohol in flower scents: Electrophysiological detection of lilac aldehyde stereoisomers by a moth. J. Chromatogr. A. 1113(1-2), 231-238.

Dötterl, S., David, A., Boland, W., Silberbauer-Gottsberger, I., Gottsberger, G., 2012. Evidence for behavioral attractiveness of methoxylated aromatics in a dynastid scarab beetle-pollinated Araceae. J. Chem. Ecol. 38(12), 1539-1543.

Dötterl, S., Jürgens, A., 2005. Spatial fragrance patterns in flowers of *Silene latifolia*: lilac compounds as olfactory nectar guides? Plant Syst. Evol. 255(1-2), 99-109.

Effmert, U., Buss, D., Rohrbeck, D., Piechulla, B., 2006. Localization of the synthesis and emission of scent compounds within the flower, in: Dudareva, N., Pichersky, E. (Eds.), Biology of Floral Scent. CRC Press, Boca Raton, FL, pp. 105-124.

Endress, P.K., 1994. Diversity and evolutionary biology of tropical flowers, first ed. New York, New York.

EPA., 1999. Citronella (oil of citronella) (021901) fact sheet. [Online.] Available from http://www.epa.gov/oppbppd1/biopesticides/ingredients/factsheets/factsheet_02190.htm

Faria, F.S., Stehmann, J.R., 2010. Reproductive biology of *Passiflora capsularis* L. e *P. pohlii* Mast. (Decaloba, Passifloracae). Act. Bot. Bras. 24(1), 262-269.

Fradin, M.S., Day, J.F., 2002. Comparative efficacy of insect repellents against mosquito bites. N. Engl. J. Med. 347, 3-18.

Friberg, M., Schwind, C., Raguso, R.A., Thompson, J.N., 2013. Extreme divergence in floral scent among woodland star species (*Lithophragma* spp.) pollinated by floral parasites. Ann. Bot. 111, 539-550.

Gibernau, M., Macquart, D., Przetak, G., 2004. Pollination in the genus *Arum*–a review. Aroideana. 27, 148-166.

Gonzalez, F., Stevenson, D.W., 2000. Perianth development and systematics of *Aristolochia*. Flora. 195(4), 370-391.

Goodrich, K.R., Raguso, R.A., 2009. The olfactory component of floral display in *Asimina* and *Deeringothamnus* (Annonaceae). New Phytologist. 183(2), 457-469.

Gottsberger, G., Silberbauer-Gottsberger, I., 1991. Olfactory and visual attraction of *Erioscelis emarginata* (Cyclocephalini, Dynastinae) to the inflorescences of *Philodendron selloum* (Araceae). Biotropica. 23(1), 23-28.

Grison-Pigé, L., Salager, J.L., Hossaert-McKey, M., Roy, J., 2001. Carbon allocation to volatiles and other reproductive components in male *Ficus carica* (Moraceae). Am. J. Bot. 88(12), 2214-2220.

Hadacek, F., Weber, M., 2002. Club-shaped organs as additional osmophores within the *Sauromatum* infloresence: odour analysis, ultrastructural changes and pollination aspects. Plant Biol. 4, 367-383.

Hall, D.W., Brown, B.V., 1993. Pollination of *Aristolochia littoralis* (Aristolochiales: Aristolochiaceae) by males of *Megaselia* spp. (Diptera: Phoridae). Ann. Entomol. Soc. Am. 86(5), 609-613.

Heiduk, A., Kong, H., Brake, I., von Tschirnhaus, M., Tolasch, T., Tröger, A.G., Wittenberg, E., Francke, W., Meve, U., Dötterl, S., 2015. Deceptive *Ceropegia dolichophylla* fools its kleptoparasitic fly pollinators with exceptional floral scent. Front. Ecol. Evol. 3(66), 1-13.

Hilje, L., 1984. Fenología y ecología floral de *Aristolochia grandiflora* Swartz (Aristolochiaceae) en Costa Rica. Brenesia. 22, 1–44.

Hipólito, J., Viana, B.F., Selbach-Schnadelbach, A., Galetto, L., Kevan, P.G., 2012. Pollination biology and genetic variability of a giant perfumed flower (*Aristolochia gigantea* Mart. And Zucc., Aristolochiaceae) visited mainly by small Diptera. Botany. 90, 815-829.

Hoballah, M.E., Stuurman, J., Turlings, T.C.J., Guerin, P.M., Connétable, S., Kuhlemeier, C., 2005. The composition and timing of flower odour emission by wild *Petunia axillaris* coincide with the antennal perception and nocturnal activity of the pollinator *Manduca sexta*. Planta. 222(1), 141-150.

Hoehne, F.C., 1942. Flora Brasilica. 15(2) Aristolochiaceae. Sao Paulo.

Howlett, F.M., 1912. The effect of oil of Citronella on two species of *Dacus*. Trans. Ent. Soc. London 60(2), 412-418.

Isman, M.B., 2000. Plant essential oils for pest and disease management. Crop Prot. 19(8), 603-608.

Janzen, D.H., 1981. Differential visitation of *Catasetum* orchid male and female flowers. Biotropica. 13(2), 77.

Johnson, S.D., 2010. The pollination niche and its role in the diversification and maintenance of the southern African flora. Phil. Trans. R. Soc. B. 365(1539), 499-516.

Johnson, S.D., Steiner, K.E., 2000. Generalization versus specialization in plant pollination systems. Trends Ecol. Evol. 15(4), 140-143

Judd, W.S., Campbell, C.S., Kellogg, E.A., Stevens, P.F., Donoghue, M.J., 2009. Sistemática Vegetal: Um Enfoque Filogenético. Porto Alegre.

Jürgens, A., Dötterl, S., Meve, U., 2006. The chemical nature of fetid floral odours in stapeliads (Apocynaceae-Asclepiadoideae-Ceropegieae). New Phytologist. 172(3), 452-468.

Jürgens, A., Wee, S.L., Shuttleworth, A., Johnson, S.D., 2013. Chemical mimicry of insect oviposition sites: a global analysis of convergence in angiosperms. Ecol. Lett. 16(9), 1157-1167.

Kaiser, R., 2006. Flowers and fungi use scents to mimic each other. Science. 311(5762), 806-807.

Kite, G.C., 1995. The floral odour of *Arum maculatum.* Biochem. Syst. Ecol. 23(4), 343-354.

Kite, G.C., Hetterscheid, W.L., 1997. Inflorescence odours of *Amorphophallus* and *Pseudodracontium* (Araceae). Phytochemistry. 46(1), 71-75.

Kite, G.C., Hetterscheid, W.L.A., Lewis, M.J., Boyce, P.C., Ollerton, J., Cocklin, E., Diaz, A., Simmonds, M.S.J., 1998. Inflorescence odours and pollinators of *Arum* and *Amorphophallus* (Araceae). Rep. Biol. Roy. Bot. Gard. Kew, 295-315.

Knudsen, J.T., Eriksson, R., Gershenzon, J., Ståhl, B., 2006. Diversity and distribution of floral scent. Bot. Rev. 72(1), 1-120.

Kolosova, N., Gorenstein, N., Kish, C.M., Dudareva, N., 2001. Regulation of circadian methyl benzoate emission in diurnally and nocturnally emitting plants. The Plant Cell. 13(10), 2333-2347.

Leonard, A.S., Dornhaus, A., Papaj, D.R., 2011. Forget-me-not: complex floral displays, inter-signal interactions, and pollinator cognition. Curr. Zool. 57(2), 215-224.

Majetic, C.J., Levin, D.A., Raguso, R.A., 2014. Divergence in floral scent profiles among and within cultivated species of *Phlox*. Sci. Hort. 172, 285-291.

Marriott, P., Shellie, R., 2002. Principles and applications of comprehensive two-dimensional gas chromatography. Trends Anal. Chem. 21(9), 573-583.

Masinde, P.S., 2004. Trap-flower fly pollination in East African *Ceropegia* L.(Apocynaceae). Int. J. Trop. Insect Sci. 24(01), 55-72.

Matile, P., Altenburger, R., 1988. Rhythms of fragrance emission in flowers. Planta. 174(2), 242-247.

Matsui, K., 2006. Green leaf volatiles: hydroperoxide lyase pathway of oxylipin metabolism. Curr. Opin. Plant Biol. 9(3), 274-280.

Meeuse, B.J., 1975. Thermogenic respiration in aroids. Annu. Rev. Plant Physiol. 26(1), 117-126.

Meeuse, B.J., Raskin, I., 1988. Sexual reproduction in the arum lily family, with emphasis on thermogenicity. Sex. Plant Reprod. 1(1), 3-15.

Milet-Pinheiro, P., Ayasse, M., Dobson, H.E., Schlindwein, C., Francke, W., Dötterl, S., 2013. The chemical basis of host-plant recognition in a specialized bee pollinator. J. Chem. Ecol. 39(11-12), 1347-1360.

Moré, M., Cocucci, A.A., Raguso, R.A., 2013. The importance of oligosulfides in the attraction of fly pollinators to the brood-site deceptive species *Jaborosa rotacea* (Solanaceae). Int. J. Plant Sci. 174(6), 863-876.

Muhlemann, J.K., Waelti, M.O., Widmer, A., Schiestl, F.P., 2006. Postpollination changes in floral odor in *Silene latifolia*: adaptive mechanisms for seed-predator avoidance? J. Chem. Ecol. 32(8), 1855-1860.

Murphy, S.M., Feeny, P., 2006. Chemical facilitation of a naturally occurring host shift by *Papilio machaon* butterflies (Papilionidae). Ecol. Monograph. 76(3), 399-414.

Murugan R., Shivanna K.R., Rao R.R., 2006. Pollination biology of *Aristolochia tagala*, a rare species of medicinal importance. Curr. Sci. 91(6), 795–798.

Nakonechnaya, O.V., Sidorenko, V.S., Koren', O.G., Nesterova, S.V., Zhuravlev, Yu.N., 2008. Specific features of pollination in the Manchurian birthwort, *Aristolochia manshuriensis*. Biol. Bull. 35(5), 459-465.

Nielsen, J.K., Jakobsen, H.B., Friis, P., Hansen, K., Møller, J., Olsen, C.E., 1995. Asynchronous rhythms in the emission of volatiles from *Hesperis matronalis* flowers. Phytochemistry. 38(4), 847-851.

van der Niet, T., Hansen, D.M., Johnson, S.D., 2011. Carrion mimicry in a South African orchid: flowers attract a narrow subset of the fly assemblage on animal carcasses. Ann. Bot. 107, 981-992.

Oelschlägel, B., Gorb, S., Wanke, S., Neinhuis, C., 2009. Structure and biomechanics of trapping flower trichomes and their role in the pollination biology of *Aristolochia* plants (Aristolochiaceae). New Phytologist. 184(4), 988-1002.

Oelschlägel, B., Nuss, M., Tschirnhaus, M., Pätzold, C., Neinhuis, C., Dötterl, S., Wanke, S., 2015. The betrayed thief–the extraordinary strategy of *Aristolochia rotunda* to deceive its pollinators. New Phytologist. 206(1), 342-351.

Ollerton, J., Masinde, S., Meve, U., Picker, M., Whittington, A., 2009. Fly pollination in *Ceropegia* (Apocynaceae: Asclepiadoideae): biogeographic and phylogenetic perspectives. Ann. Bot. 103(9), 1501-1514.

Pearson, D.L., Dressler, R.L., 1985. Two-year study of male orchid bee (Hymenoptera: Apidae: Euglossini) attraction to chemical baits in lowland south-eastern Peru. J. Trop. Ecol. 1, 37-54.

Petch, T., 1924. Notes on *Aristolochia*. Ann. Roy. Bot. Gard. (Peradeniya). 8, 1-109.

Prieto-Benítez, S., Dötterl, S., Giménez-Benavides, L., 2015. Diel variation in flower scent reveals poor consistency of diurnal and nocturnal pollination syndromes in Sileneae. J. Chem. Ecol. 41(12), 1095-1104.

Policha, T., Davis, A., Barnadas, M., Dentinger, B., Raguso, R.A., Roy, B.A., 2016. Disentangling visual and olfactory signals in mushroom-mimicking *Dracula* orchids using realistic three-dimensional printed flowers. New Phytologist. 210(3), 1058-1071.

Proctor, M., Yeo, P., Lack, A., 1996. The natural history of pollination. London, UK.

Proffit, M., Schatz, B., Bessière, J.M., Chen, C., Soler, C., Hossaert-McKey, M., 2008. Signalling receptivity: comparison of the emission of volatile compounds by figs of *Ficus hispida* before, during and after the phase of receptivity to pollinators. Symbiosis. 45, 15-24.

Raguso, R.A., 2008. Wake up and smell the roses: the ecology and evolution of floral scent. Annu. Rev. Ecol. Evol. Syst. 39, 549-569.

Raguso, R.A., Levin, R.A., Foose, S.E., Holmberg, M.W., McDade, L.A., 2003. Fragrance chemistry, nocturnal rhythms and pollination "syndromes" in *Nicotiana*. Phytochemistry. 63(3), 265-284.

Raguso, R.A., Weiss, M.R., 2015. Concerted changes in floral colour and scent, and the importance of spatio-temporal variation in floral volatiles. J. Indian. Inst. Sci. 95(1), 69-92.

Raskin, I., Turner, I.M., Melander, W.R., 1989. Regulation of heat production in the inflorescences of an *Arum* lily by endogenous salicylic acid. Proc. Nat. Acad. Sci. 86(7), 2214-2218.

Razzak, M.A., Ali, T., Ali, S.I., 1992. The pollination biology of *Aristolochia bracteolate* Lamk. (Aristolochiaceae). Pakistan J. Bot. 24(1) 79-87.

Renner, S.S., 2006. Rewardless flowers in the angiosperms and the role of insect cognition in their evolution, in: Waser, N.M., Ollerton, J. (Eds.), Plant-Pollinator Interactions: From Specialization to Generalization. The University of Chicago Press, Chicago, pp. 123-144.

Robroek, B.J., de Jong, H., Arce, H., Sommeijer, M.J., 2003a. The development of *Pseudohypocera kerteszi* (Diptera, Phoridae), a kleptoparasite in nests of stingless bees (Hymenoptera, Apidae) in Central America. Proc. Exp. App. Entomol. 14, 71-74.

Robroek, B.J., de Jong, H., Sommeijer, M.J., 2003b. The behaviour of the kleptoparasite, *Pseudohypocera kerteszi* (Diptera, Phoridae), in hives of stingless bees (Hymenoptera, Apidae) in Central America. Proc. Exp. App. Entomol. 14, 65-70.

Rulik, B., Wanke, S., Nuss, M., Neinhuis, C., 2008. Pollination of *Aristolochia pallida* Willd. (Aristolochiaceae) in the Mediterranean. Flora. 203(2), 175-184.

Sakai, S., 2002. A review of brood-site pollination mutualism: plants providing breeding sites for their pollinators. J. Plant. Res. 115(3), 0161-0168.

Schlumpberger, B.O., Raguso, R.A., 2008. Geographic variation in floral scent of *Echinopsis ancistrophora* (Cactaceae); evidence for constraints on hawkmoth attraction. Oikos. 117(6), 801-814.

Shabby, A.S., El-Gengaihi, S., Khattab, M., 1995. Oil of *Melissa officinalis* L., as affected by storage and herb drying. J. Essent. Oil Res. 7(6), 667-669.

Shuttleworth, A., Johnson, S.D., 2009. The importance of scent and nectar filters in a specialized wasp-pollination system. Funct. Ecol. 23(5), 931-940.

Shuttleworth, A., Johnson, S.D., 2010. The missing stink: sulphur compounds can mediate a shift between fly and wasp pollination systems. Proc. R. Soc. B. 277, 2811-2819.

Sinn, B.T., Kelly, L.M., Freudenstein, J.V., 2015. Putative floral brood-site mimicry, loss of autonomous selfing, and reduced vegetative growth are significantly correlated with increased diversification in *Asarum* (Aristolochiaceae). Mol. Phylogenet. Evol. 89, 194-204.

Skubatz, H., Kunkel, D.D., Howald, W.N., Trenkle, R., Mookherjee, B., 1996. The *Sauromatum guttatum* appendix as an osmophore: excretory pathways, composition of volatiles and attractiveness to insects. New Phytologist. 134(4), 631-640.

Smith, B.N., Meeuse, B.J., 1966. Production of volatile amines and skatole at anthesis in some *Arum* lily species. Plant Physiol. 41(2), 343-347.

Stensmyr, M.C., Urru, I., Collu, I., Celander, M., Hansson, B.S., Angioy, A.M., 2002. Pollination: Rotting smell of dead-horse arum florets. Nature. 420(6916), 625-626.

Stökl, J., Strutz, A., Dafni, A., Svatos, A., Doubsky, J., Knaden, M., Sachse, S., Hansson, B.S. Stensmyr, M.C., 2010. A deceptive pollination system targeting drosophilids through olfactory mimicry of yeast. Curr. Biol. 20(20), 1846-1852.

Terry, L.I., Roemer, R.B., Walter, G.H., Booth, D., 2014. Thrips' responses to thermogenic associated signals in a cycad pollination system: the interplay of temperature, light, humidity and cone volatiles. Funct. Ecol. 28(4), 857-867.

Terry, I., Walter, G.H., Moore, C., Roemer, R., Hull, C., 2007. Odor-mediated push-pull pollination in cycads. Science. 318(5847), 70.

Theis, N., Raguso, R.A., 2005. The effect of pollination on floral fragrance in thistles. J. Chem. Ecol. 31(11), 2581-2600.

Trujillo, C.G., Sérsic, A.N., 2006. Floral biology of *Aristolochia argentina* (Aristolochiaceae). Flora. 201(5), 374-382.

Underwood, B.A., Tieman, D.M., Shibuya, K., Dexter, R.J., Loucas, H.M., Simkin, A J., Sims, C.A., Schmelz, E.A., Klee, H.J., Clark, D.G., 2005. Ethylene-regulated floral volatile synthesis in petunia corollas. Plant Physiol. 138(1), 255-266.

Urru, I., Stensmyr, M.C., Hansson, B.S., 2011. Pollination by brood-site deception. Phytochemistry. 72(13), 1655-1666.

Vogel, S., 1963. Duftdrüsen im Dienste der Bestäubung. Über Bau und Funktion der Osmophoren. Abh. Math.-Naturwiss. Kl. Akad. Wiss. Mainz 10, 600-763.

Vogel, S., 1978. Pilzmückenblumen als Pilzmimeten. Flora. 167, 329–398.

Vogel, S., 1990. The Role of Scent Glands in Pollination : On the Structure and Function of Osmophores. Washington, DC.

Wagner, S.T., Hesse, L., Isnard, S., Samain, M-S., Bolin, J., Maass, E., Neinhuis, C., Rowe, N.P., Wanke, S., 2014. Major trends in stem anatomy and growth forms in the perianth-bearing Piperales, with special focus on *Aristolochia*. Ann. Bot. 113(7), 1139-1154.

Wolda, H., Sabrosky, C.W., 1986. Insect visitors to two forms of *Aristolochia pilosa* in Las Cumbres, Panama. Biotropica. 18(4), 295-299.

Wright, G.A., Schiestl, F.P., 2009. The evolution of floral scent: the influence of olfactory learning by insect pollinators on the honest signalling of floral rewards. Funct. Ecol. 23(5), 841-851.
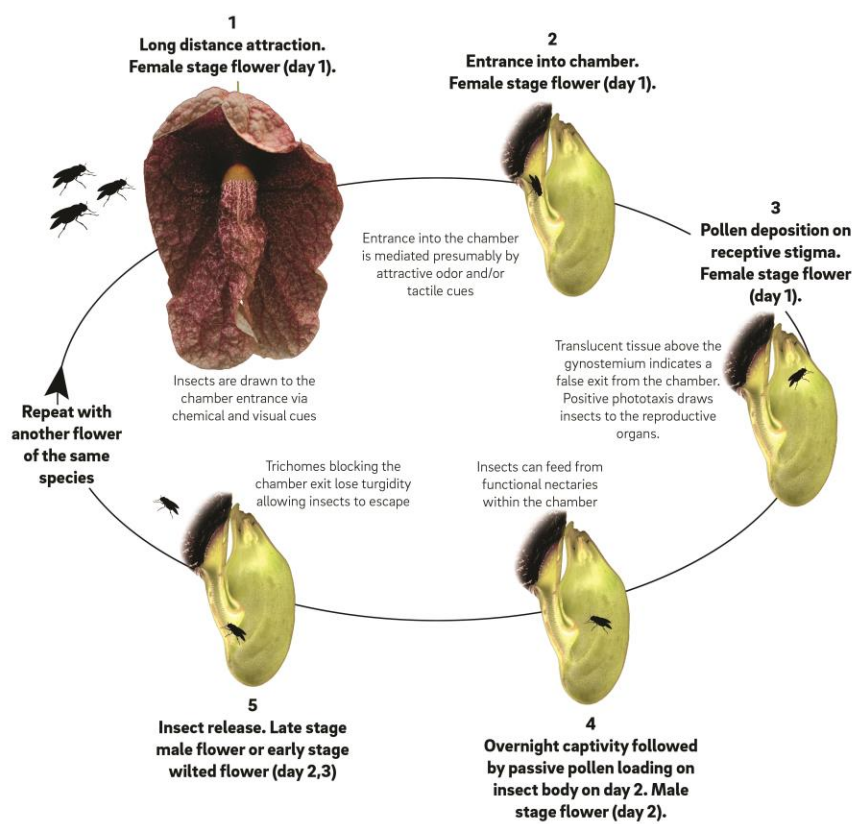
Figure 1. The sequence of pollinator imprisonment for flowers of *Aristolochia gigantea.*
(1) Pollinators and other visitors are attracted to the female stage flowers via chemical
and other cues on the first day of anthesis. White striations on a red background resemble
the appearance of flesh while the contrast of a bright yellow spot on a black background
provides a visual cue for orientation to the chamber entrance. (2) To enter into the
chamber, visitors must traverse a floral tube lined with downward facing trichomes which
simultaneously prevent them from leaving. (3) For pollination to be successful, visitors
must be carrying pollen from a conspecific flower to deposit on the receptive stigma
located at the basal end of the chamber. A pellucid zone of tissue or "window pane"
above the gynostemium allows sunlight into the chamber indicating a false exit from the
trap. Positive phototaxis draws the insects near the gynostemium allowing pollen to be
passively deposited on the stigmatic surface. (4) Insects must remain captive overnight to
receive pollen from the dehiscent anthers on the second day of anthesis. A food source is
provided by two patches of glandular hairs within the chamber which function as
nectaries. As sunlight passes through the window pane on day 2, the insects are drawn
near the reproductive organs again and are loaded with pollen in the process. (5) As the
flowers begin to senesce on late day 2 or on early day 3 the trichomes that were once
blocking the exit from the trap lose their turgidity and allow the insects to escape. Cross
pollination is achieved when insects bearing pollen are deceived again by another female
A. gigantea flower.
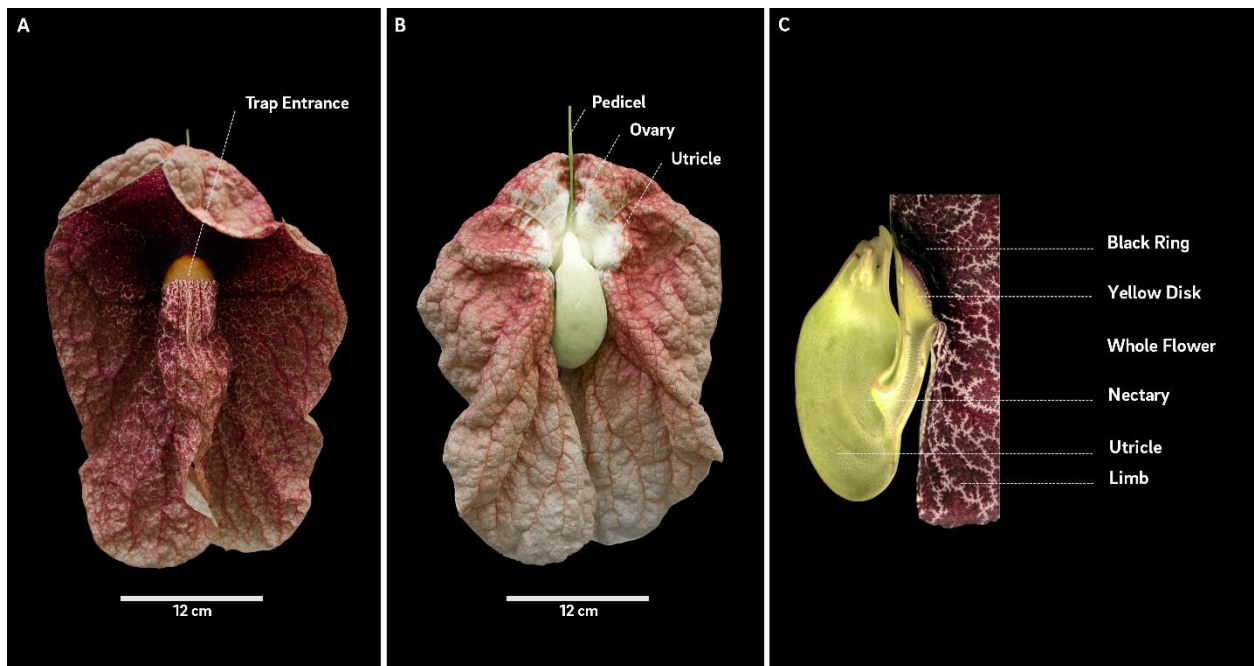
Figure 2. (A) Anterior view of the *Aristolochia gigantea* var. *brasiliensis* limb showing a red and white striated visual display, with a black and yellow zone of tissue (referred to as black ring and yellow disk in this paper) near the entrance of the floral tube leading to the floral chamber. (B) Posterior view of the *Aristolochia gigantea* var. *brasiliensis* flower indicating the placement of the floral chamber (utricle). At the basal end of the utricle extends the ovary leading to the pedicel. (C) A cross section through the flower with labels indicating the spatial units from which volatiles were sampled at each ontogenic stage of floral development (female stage, male stage, wilted stage).
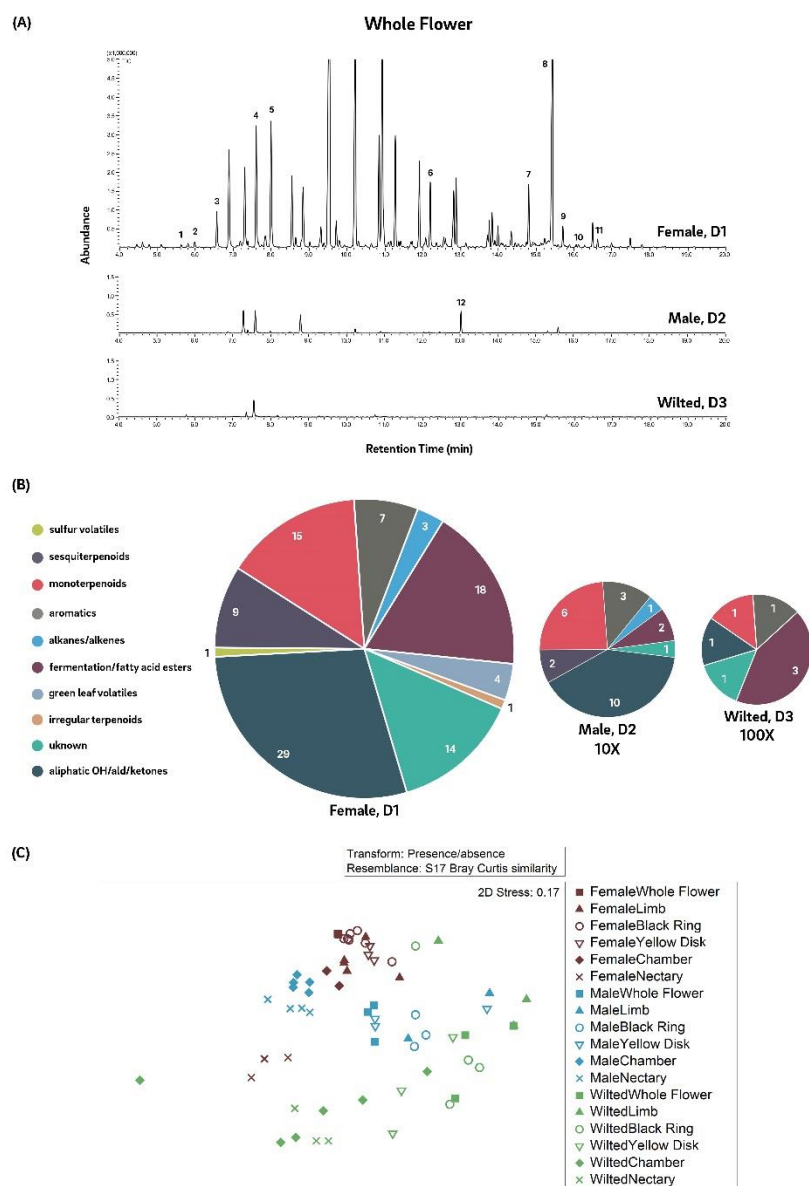
Figure 3. (A) GC-MS total ion chromatograms of volatiles collected from *Aristolochia gigantea* whole flowers at distinct ontogenic stages of floral development (female, day 1; male, day 2; wilted, day 3). Female stage flowers emit a highly complex blend of volatiles including a simultaneous (and paradoxical) emission of brood-site associated compounds (dimethyl disulfide (**1**), 3-methyl-2-butanol (**2**), 3-methyl-1-butanol acetate (**3**), 2-heptanone (**4**), 3-methyl-1-butanol (**5**)) and sweet citrus associated compounds (citronellal (**6**), (*Z*)-citral (neral) (**7**), (*E*)-citral (geranial) (**8**), citronellol (**9**), nerol (**10**), geraniol (**11**)). Volatile emission is highly reduced in male stage flowers except for the novel production of linalool (**12**) during this stage. After three days, wilted flowers nearly cease volatile emission altogether and chemically resemble the vegetative background. For structures see Fig. S4.

42

(B) Pie charts depicting the number of volatiles produced within each designated compound class as a proportion relative to the total number of volatiles produced by intact whole flowers at each stage of development (female whole flowers = 101 total compounds, male whole flowers = 25 total compounds, wilted whole flowers = 7 total compounds). Numbers within the pie wedges represent the number of volatiles produced within each designated compound class. Pie chart areas are scaled to depict the total relative volatile emission (based on average total peak area) by whole flowers at each stage. Male whole flower and wilted whole flower pie chart areas are shown at 10X and 100X magnification respectively because they are too small for proper viewing at 1X magnification (male 2% total scent emission relative to female, wilted 0.14% total scent emission relative to female).

(C) Multidimensional (MDS) scaling plot constructed using the Bray-Curtis similarity index showing the relationship of floral volatile composition between each *Aristolochia gigantea* stage-part combination sampled. Flower stage is grouped by color (female = maroon, male = pale blue, wilted = green), while the same floral parts across all floral stages share the same symbol (square = whole flower, upside triangle = limb, circle = black ring, downside triangle = yellow disk, diamond = utricle, cross = nectary).
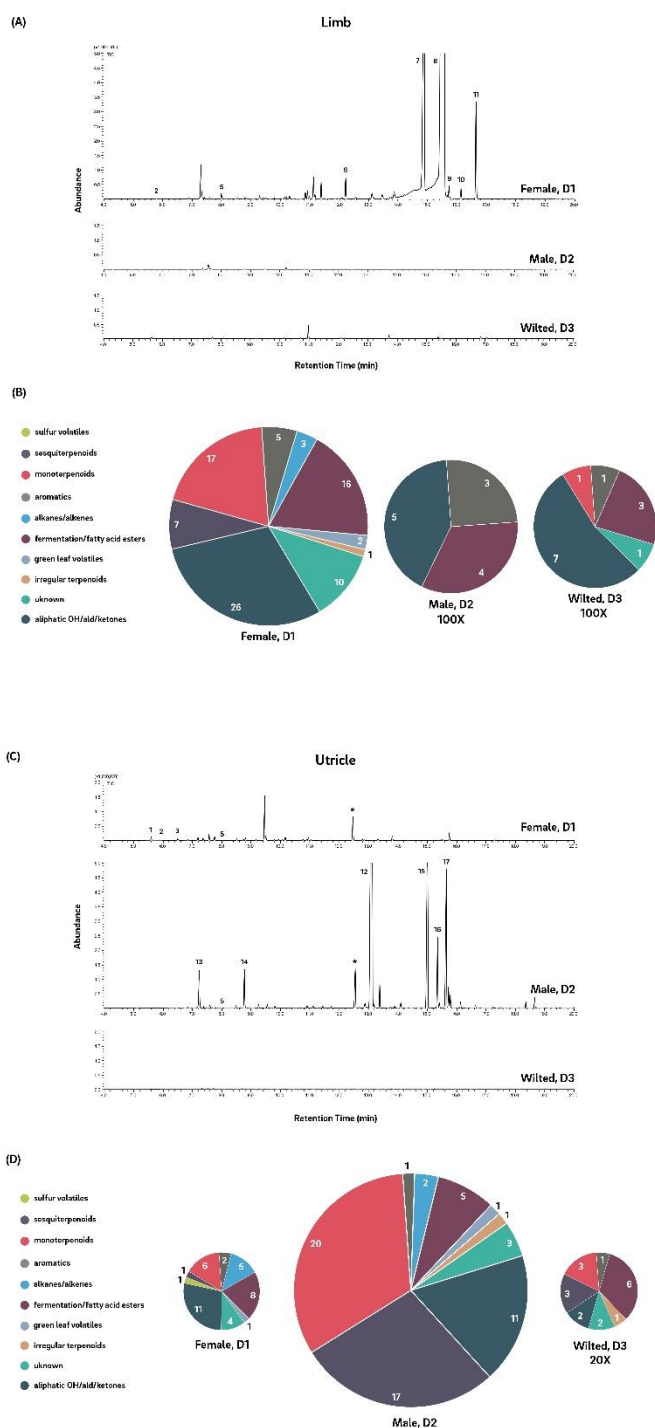
Figure 4. (A) GC-MS total ion chromatograms of volatiles collected from dissected *Aristolochia gigantea* limbs at distinct ontogenic stages of development. Strong emission of sweet citrus associated compounds (citronellal (**6**), (*Z*)-citral (neral) (**7**), (*E*)-citral (geranial) (**8**), citronellol (**9**), nerol (**10**), geraniol (**11**)) is specific to the female stage limb. Several brood-site associated compounds (3-methyl-2-butanol (**2**), 3-methyl-1-butanol (**5**)) are also produced by the female limb at this time point. Both male stage

44

flowers and wilted stage flowers show highly reduced volatile emission and chemically resemble the vegetative background. For structures see Fig. S4.

(B) Pie charts depicting the number of volatiles produced within each designated compound class as a proportion relative to the total number of volatiles produced by the limb at each stage of development (female limb = 87 total compounds, male limb = 12 total compounds, wilted limb = 13 total compounds). Pie chart areas are scaled to depict the total relative volatile emission by the limb at each stage. Male limb and wilted limb pie chart areas are each shown at 100X magnification because they are too small for proper viewing at 1X magnification (male 0.44% total scent emission relative to female, wilted 0.36% total scent emission relative to female).

(C) GC-MS total ion chromatograms of volatiles collected from dissected *Aristolochia gigantea* utricles at distinct ontogenic stages of floral development. Volatile emission of the female stage utricle is weak yet diverse including brood-site associated volatiles (dimethyl disulfide (**1**), 3-methyl-2-butanol (**2**), 3-methyl-1-butanol acetate (**3**), 3-methyl-1-butanol (**5**)), several branched chain esters, and various monoterpenes and sesquiterpenes. By day two the male stage utricle ceases production of brood-site associated volatiles (except for 3-methyl-1-butanol) and produces an intense emission of linalool (**12**), methyl geranate (**15**), (*Z,E*)-α-farnesene (**16**), and (*E,E*)-α-farnesene (**17**) as well as increased emission of β-myrcene (**13**) and (*E*)-β-ocimene (**14**). After three days, wilted utricles nearly cease volatile emission altogether and chemically resemble the vegetative background. Asterisks indicate ambient contaminants. For structures see Fig. S4.

(D) Pie charts depicting the number of volatiles produced within each designated compound class as a proportion relative to the total number of volatiles produced by the utricle at each stage of development (female utricle = 39 total compounds, male utricle = 61 total compounds, wilted utricle = 18 total compounds). Pie chart areas are scaled to depict the total relative volatile emission by the utricle at each stage. The wilted utricle pie chart area is shown at 20X magnification because it is too small for proper viewing at 1X magnification (female 11% total scent emission relative to male, wilted 0.56% total scent emission relative to male).

Table 1. A heat map as a visual representation of individual gas-chromatographic peak areas of volatiles across all floral stages and units sampled. Columns are organized from left to right by flower stage (female, male, wilted, bud) with each stage including all dissected floral units (see Fig. 2C). Compounds in rows are assigned into chemical classes and grouped by retention time and corresponding Kovats Retention Index in ascending order. Blue color shading is based on a log scale of peak area with the lightest blue shade spanning two log increments (1-10,000 units) and white space representing no volatile production. Identification of compounds was based on: bold = comparison with authentic standards, * = comparison to published Kovats Indices, not bold = a 90% or greater match with mass spectral library, mass spectral fragments = when none of the above criteria were satisfied.

Top column group headers: **Female** | **Male** | **Wilted** | **Bud**
Sub-columns under each group: Whole Flower, Limb, Black Ring, Yellow Disk, Chamber, Nectary (Bud: Whole Flower, Chamber)

Key — Abundance
- 0
- 1 – 10,000
- 10,001 – 100,000
- 100,001 – 1,000,000
- 1,000,001 – 10,000,000
- 10,000,001 – 100,000,000

Compound Class	Compound Name	RT (min)	KRI
aliphatic alcohols / aldehydes / ketones	3-methyl-2-butanone	3.179	915
	2-pentanone	3.894	963
	4-methyl-2-pentanone	4.431	1011
	3-methyl-2-pentanone*	4.576	1007
	2-hexanone*	5.721	1071
	3-pentanol*	6.446	1112
	2-pentanol*	6.702	1127
	5-methyl-2-hexanone*	6.886	1137
	40,41,42,43,44,53,55,69,70,98	7.104	1150
	2-methyl-4-pentenal	7.181	1154
	2-heptanone	7.587	1177
	heptanal*	7.659	1181
	40,41,43,44,45,55,56,57,71,85	7.804	1190
	4-hepten-2-one	8.491	1232
	6-methyl-2-heptanone*	8.563	1236
	41,42,43,44,55,57,58,59,70,71	8.858	1255
	40,41,42,43,44,55,56,57,69	9.133	1273
	41,42,43,44,45,55,56,57,69,70	9.172	1275
	2-octanone*	9.327	1285
	octanal*	9.404	1290
	4-methyl-1-pentanol*	9.723	1310
	2-heptanol	9.81	1316
	40,41,42,44,55,56,57,69,70,83	9.979	1326
	40,41,43,44,45,55,56,69,70,73	10.023	1329
	41,42,43,55,56,57,69,70,83,97	10.081	1333
	41,42,43,55,57,58,59,71,82,84	10.24	1343
	40,41,43,44,55,57,71,72	10.313	1348
	4-methyl-3-penten-1-ol*	10.864	1384
	2-nonanone*	10.97	1390
	3-methyl-1-hexanol	11.178	1404
	4-methyl-1-hexanol*	11.434	1422
	41,43,44,53,55,58,67,69,71,82	11.705	1441
	2-methylpentanal	11.739	1444
	41,42,43,55,56,57,68,69,70,84	12.575	1503
	41,43,44,45,55,56,57,60,69,70	12.657	1509
	40,41,43,44,55,56,58,59,69,71	13.029	1536
	41,42,43,44,55,56,57,58,69,70	13.15	1544
	2-undecanone*	13.774	1589
	41,43,44,53,54,55,67,69,81,110	14.358	1637
	2-tridecanone*	16.301	1796
aliphatic fermentation related compounds / fatty acid esters	ethyl isovalerate	5.557	1062
	3-methyl-2-butanol	6.011	1088
	3-methyl-1-butyl acetate*	6.548	1118
	3-methylbutyl propionate*	7.746	1186
	3-methyl-1-butanol	8.017	1202
	3-methylbutyl butyrate*	9.037	1266
	acetoin	9.308	1284
	3-methylbutyl 3-methylbutanoate*	9.482	1295
	3-methyl-3-butenyl isovalerate	10.656	1370
	2-butoxyethanol*	11.052	1396
	41,42,43,55,56,69,70,71,81,99	11.294	1412
	3-methylbutyl hexanoate*	11.932	1458
	41,42,43,44,55,69,70,71,87,95	12.614	1506
	41,42,43,55,57,69,70,71,95,113	12.812	1520
	41,42,43,55,56,57,69,70,71,109	13.914	1599
	41,42,43,54,55,67,68,69,81,82	14.102	1615
	41,43,44,54,55,58,67,68,69,81	14.146	1619
	41,43,53,55,67,69,79,81,93,108	14.929	1686
	41,43,54,55,58,67,68,81,82,96	16.509	1820
	isopropyl dodecanoate*	16.537	1823
	40,41,43,44,55,56,57,71,73,89	16.843	1860
	41,43,44,45,55,57,70,71,91,105	16.886	1866
	40,41,43,44,55,56,57,71,83,89	17.055	1886
	41,43,45,54,55,58,67,71,81,82	17.814	1951
	isopropyl myristate*	18.602	2016
	isopropyl palmitate	20.603	2217
	40,41,43,44,45,55,67,82,83,96	21.468	2310
aliphatic green leaf volatiles	3-hexanol	7.843	1192
	1-hexanol	10.313	1348
	40,41,43,44,55,57,58,67,69,82	11.507	1427
	40,41,43,44,45,55,58,67,69,82	11.613	1435
	40,41,43,44,55,67,69,81,82,97	15.315	1718
alkanes / alkenes	undecane	5.847	1078
	dodecane	7.761	1187
	tridecane	9.525	1297
	40,41,43,44,55,57,71,85	10.569	1364
	41,43,44,55,56,57,58,69,71,85	11.091	1398
	40,41,43,44,55,57,67,68,81,95	13.208	1549
	41,43,55,56,69,70,71,82,83,110	14.006	1607
	41,42,43,44,55,56,57,69,70,97	14.088	1614
	40,41,43,44,53,55,67,69,79,81	16.161	1785
	40,41,44,53,55,67,69,79,81,93	16.195	1788
	nonadecane	17.302	1910
	heneicosane	19.371	2090
aromatics	styrene*	8.747	1248
	anisole	10.255	1344
	benzyl methyl ether	10.985	1391
	phenylacetaldehyde	14.281	1631
	acetophenone*	14.47	1647
	benzyl alcohol	17.017	1882
	benzyl isovalerate	17.254	1907
	3-methylbutyl benzoate*	17.51	1927
	3-methylbutyl phenylacetate	18.418	1998
irregular terpenoids	6-methyl-5-hepten-2-one	10.168	1339

47

Compound Class	Compound Name	RT (min)	KRI	Female						Male						Wilted						Bud	
				Whole Flower	Limb	Black Ring	Yellow Disk	Chamber	Nectary	Whole Flower	Limb	Black Ring	Yellow Disk	Chamber	Nectary	Whole Flower	Limb	Black Ring	Yellow Disk	Chamber	Nectary	Whole Flower	Chamber
monoterpenoids	3-carene	6.93	1140																				
	α-phellandrene	7.234	1157																				
	β-myrcene	7.282	1160																				
	α-terpinene	7.379	1165																				
	40,41,43,44,51,53,77,79,91,105,107,1	8.196	1213																				
	cis-β-ocimene*	8.413	1227																				
	trans-β-ocimene	8.829	1253																				
	p-cymene	9.056	1268																				
	α-terpinolene*	9.303	1283																				
	41,43,53,55,69,79,91,95,135,150	11.13	1401																				
	41,43,53,55,69,79,91,95,135,150 #2	11.386	1419																				
	trans-linalool oxide (furanoid)	11.555	1431																				
	40,41,51,55,65,77,79,91,119,134	11.717	1442																				
	cis-linalool oxide (furanoid)	11.956	1459																				
	40,41,44,45,55,67,69,70,81,83	11.961	1460																				
	citronellal	12.217	1478																				
	41,42,43,44,53,55,68,69,70,71	12.899	1526																				
	linalool	13.024	1535																				
	41,43,54,55,67,68,69,81,82,95	13.368	1560																				
	40,41,43,44,55,59,68,94	14.025	1609																				
	methyl nerolate	14.209	1624																				
	(Z)-citral (neral)	14.832	1678																				
	methyl geranate	14.963	1689																				
	(E)-citral (geranial)	15.456	1729																				
	citronellol	15.726	1751																				
	nerol	16.137	1783																				
	40,41,43,44,55,67,68,69,91,93	16.21	1789																				
	geraniol	16.64	1836																				
sesquiterpenoids	β-elemene	13.725	1586																				
	41,43,53,55,67,69,79,91,93,121	14.334	1635																				
	(Z)-β-farnesene	14.494	1649																				
	41,43,55,69,77,79,91,93,105,161	14.648	1662																				
	40,41,43,55,67,69,79,81,91	14.982	1691																				
	41,43,53,55,67,69,81,91,161,189	15.001	1692																				
	41,43,53,55,69,79,81,91,105,161	15.141	1704																				
	(Z,E)-α-farnesene*	15.315	1718																				
	(E,E)-α-farnesene*	15.591	1740																				
	41,55,77,81,91,105,119,134,161,204	15.789	1756																				
	41,43,55,69,91,105,133,161,189,204	15.9	1764																				
	40,41,44,55,77,79,91,93,105,107	15.924	1766																				
	41,43,55,67,69,91,105,107,122,161	16.074	1778																				
	40,41,43,44,53,55,67,91,93,121	16.524	1822																				
	41,43,55,69,77,79,91,93,107,135 (isor	17.239	1906																				
	41,43,55,69,77,79,91,93,107,135 (isor	17.476	1924																				
	41,43,53,55,59,79,81,91,93,119	18.351	1993																				
	41,43,55,59,79,80,81,91,93,119	18.655	2021																				
	40,41,43,44,67,69,81,95,109,123	18.882	2043																				
	41,42,43,44,55,67,69,81,95,123	20.004	2155																				
	41,43,53,55,67,69,81,82,114,121	20.463	2202																				
	41,43,44,45,53,55,67,69,81,95	20.927	2251																				
	41,53,55,67,68,79,81,93,107,121	20.946	2253																				
	41,43,45,53,55,77,79,81,91,93	21.695	2336																				
	41,43,55,67,79,81,91,119,133	22.155	2387																				
	41,43,53,55,67,79,81,91,93,121	22.232	2396																				
sulfur volatiles	dimethyl disulfide	5.596	1064																				
unknown	41,42,43,45,53,55,58,67,68,69,82,86	4.75	1017																				
	41,42,43,44,45,56,57,58,69,72	5.074	1035																				
	41,42,43,44,45,55,56,57,68,82	8.665	1243																				
	40,41,43,44,45,55,57,69,70,87	8.935	1260																				
	cyclopentanol*	9.438	1292																				
	41,42,43,44,55,56,57,59,67,69	10.381	1352																				
	40,41,42,43,44,53,55,58,67,69	10.472	1358																				
	41,42,43,44,45,55,56,57,69,95	10.501	1360																				
	41,42,43,45,53,55,69,70,81,83	12.096	1469																				
	40,41,43,44,55,55,57,70,72,83	12.188	1476																				
	40,41,43,44,55,56,57,69,70,83	12.662	1509																				
	41,43,55,56,59,69,70,97,114,115	12.836	1522																				
	41,43,53,55,67,69,81,94,109	13.111	1542																				
	41,42,43,44,53,55,57,69,71,93	13.247	1551																				
	40,41,43,44,45,55,67,69,81,94 (isome	13.45	1566																				
	40,41,43,44,45,55,69,70,81,91 (isome	13.542	1573																				
	41,43,55,67,77,79,80,81,93,108	14.078	1613																				
	41,42,43,44,45,53,55,67,69,84	15.185	1707																				
	41,43,44,45,55,69,71	16.79	1854																				

Key

Abundance
- 0
- 1 - 10,000
- 10,001 - 100,000
- 100,001 - 1,000,000
- 1,000,001 - 10,000,000
- 10,000,001 - 100,000,000